Photoelectron Imaging Spectroscopy of Small Clusters: Evidence for Non-Boltzmannian Kinetic-Energy Distribution in Thermionic Emission

J. C. Pinaré, B. Baguenard, C. Bordas, and M. Broyer
Laboratoire de Spectrométrie Ionique et Moléculaire, Université Claude Bernard Lyon 1 and CNRS, Bâtiment 205,
43 Boulevard du 11 Novembre 1918, F69622 Villeurbanne Cedex, France

(Received 8 April 1998)

The competition between thermionic emission and direct photoelectron emission has been measured in small tungsten clusters using photoelectron imaging spectroscopy. The kinetic energy distribution of electrons corresponding to thermionic emission is found to vary as $p(\epsilon) \propto \epsilon^{1/2}\exp(-\epsilon/kT)$, in agreement with theoretical predictions, and does not follow the bulklike function $p(\epsilon) \propto \epsilon\exp(-\epsilon/kT)$ or the simple exponentially decreasing Boltzmann function $p(\epsilon) \propto \exp(-\epsilon/kT)$, as usually assumed in photoelectron spectroscopy of clusters. Moreover, the angular distribution of direct photoelectrons is observed and the evolution as a function of the size is discussed. [S0031-9007(98)07082-3]

PACS numbers: 36.40.–c, 33.60.Cv

The optical excitation of a molecule, cluster, or solid by absorption of one or several photons results in a decay process that follows different channels (emission of atom, molecule, electron, photon...) according to the size of the particle and its internal energy. When the excess energy is sufficient to remove an electron or atom from the system, the emission of a photon is usually negligible. In negative clusters of refractory elements such as tungsten [1–6], niobium [7], or fullerenes [8–12], the energy required to remove an electron is significantly lower than the energy required to remove an atom. For example, in small negative tungsten clusters W_n^- $(n < 15)$ the electron affinity (EA) is less than 2 eV [4] while the bulk heat of vaporization is about 8.9 eV/atom. In this paper, we focus on the case where the absorption of a single photon of energy $h\nu$ is sufficient to remove an electron from a finite size negatively charged system: $h\nu >$ EA. As model systems, we study the photodetachment of W_n^- clusters $(n < 12)$ by single-photon excitation. Neutral [1–3] and negative tungsten clusters [4–6] have already been extensively studied and the kinetic-energy distribution of photoelectrons has been measured [4,5]. However, our specific experimental setup allows us to study the photoelectron spectrum near threshold which is extremely different in a finite size system as compared to the bulk matter. These clusters, excited above the detachment threshold and below the dissociation threshold, may decay only by electronic emission. The excited state can lead directly to the emission of a photoelectron. This corresponds to direct photoemission (DPE): The excess energy is converted to photoelectron kinetic energy $\epsilon = h\nu - E_f$ (E_f energy of the final state of the target). The corresponding kinetic energy photoelectron spectrum mirrors the target excited state spectrum. Before decay, the excited electron may also transfer part of its energy to the nuclei. In a cluster, owing to the combination of a limited number of degrees of freedom and of a large density of states, this kind of indirect process leads to thermionic emission (TE) [13] while in bulk matter this results in inelastic photoelectron scattering [14]. In bulk matter, TE corresponds to the ejection of electrons from a surface at temperature T with a kinetic energy distribution described by

$$p(\epsilon) \propto \epsilon \exp(-\epsilon/kT)\,, \tag{1}$$

where k is the Boltzmann constant. Indirect decay channels in clusters are comparable, and electron-vibration couplings result in a thermalization process which leads to a high internal temperature owing to the limited number of vibrational degrees of freedom. However, the bulklike function [Eq. (1)] is not relevant to finite size systems. The detailed theoretical aspects of TE of clusters has been extensively studied by Klots and co-workers [15,16]. These studies show that the kinetic energy distribution $p(\epsilon)$ of thermal electrons in the limit of small size particles is dominated by a term proportional to $\exp(-\epsilon/kT)$ for neutral or positively charged systems while it is dominated by a term proportional to $[\epsilon^{1/2}\exp(-\epsilon/kT)]$ for negative species. We present here the first experimental results obtained in the photodetachment of small negative clusters which exhibit without ambiguity a behavior departing significantly from Eq. (1).

Standard photoelectron spectroscopy techniques such as the magnetic bottle spectrometer [17] are not appropriate for studying the kinetic energy distribution of low energy photoelectrons below 0.2 eV. In order to observe slow electrons, we use a recent evolution of the photoelectron imaging spectroscopy [18–20]: velocity map imaging [21,22]. Our experimental setup, described in detail elsewhere [23], is briefly as follows. The negatively charged clusters are produced in a laser vaporization source seeded with helium which cools the clusters below 300 K. The anions are extracted from the cluster beam in the extraction region of a Wiley-McLaren time-of-flight mass spectrometer (TOFMS) by a pulsed electric field. The photoelectron imaging spectrometer is located at the end of the TOFMS drift tube and the excitation of a given cluster size is ensured by a proper delay between the pulsed extraction and firing of the photodetachment laser (XeCl excimer laser, $\lambda = 308\,\text{nm}$). A static electric field is applied in the photoelectron spectrometer to project the photoelectrons onto a position sensitive detector. This results in an image which is the superposition of circular rings of radius proportional to the initial velocity with a filling pattern that reveals the original angular distribution with respect to the laser polarization. After inversion [20], the image gives the initial energetic and angular distribution of the photoelectrons. Velocity map imaging allows mapping of all electrons with the same initial velocity, irrespective of their initial position, and allows us to work with a relatively large cluster beam/laser interaction zone (5 mm diameter) without degrading the image resolution.

Figure 1 presents a typical photoelectron image of W_5^- at $\lambda = 308$ nm. Two specific advantages of imaging are clearly visible on this figure. First, as opposed to other photoelectron spectroscopy techniques, the efficiency of the imaging spectrometer is independent of the kinetic energy of the photoelectron. This allows us to detect the broad slow thermal electron distribution visible in the center of the image. Second, this method is sensitive to the angular distribution. In DPE, the photoelectron angular distribution is usually anisotropic and depends on the angular couplings in the initial and final states of the target. However, in TE, the initial orientation is lost during the internal energy redistribution process, and the thermal electron emission is isotropic. This last feature is clearly visible in the image. The broad central isotropic thermal distribution is surrounded by anisotropic (more intense along the laser polarization axis) and sharper features which correspond to DPE from d-orbitals. According to Ref. [15], the kinetic energy distribution of TE of a cluster of N atoms of radius R_N ($R_N = r_s N^{1/3}$ with r_s the Wigner-Seitz radius) may be expressed as

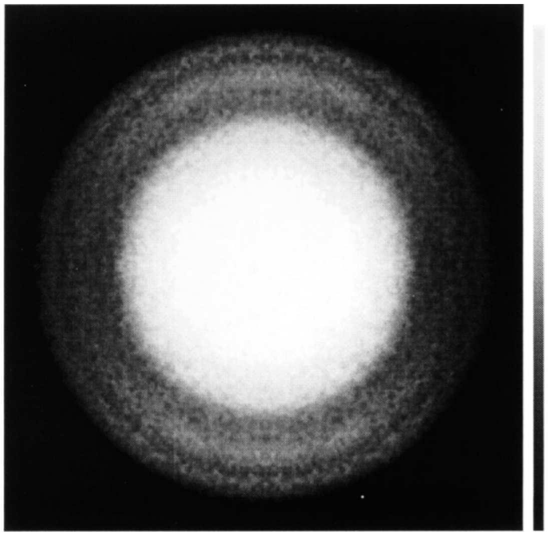

FIG. 1. Typical photoelectron image of W_5^- at $\lambda = 308$ nm. Laser polarization is oriented along the vertical axis. The isotropic slow thermal electron distribution is visible in the center of the image. It is surrounded by anisotropic and sharper features corresponding to direct photoemission.

$$p(\epsilon) \propto \{1 - \exp[-BL_{\max}^2(\epsilon)/kT]\}\exp(-\epsilon/kT)\,, \quad (2)$$

with T the internal temperature of the system defined by (the initial temperature of the cluster, $T_0 < 300\,\text{K}$, is neglected)

$$T = \frac{h\nu}{(3N - 6)k}\,. \quad (3)$$

The maximum value of the angular momentum $L_{\max}$ of the outgoing electron may be written, for a negatively charged system (only polarization long-range potential), as

$$L_{\max}^2(\epsilon) = \left(\frac{2\mu}{\hbar^2}\right)[(2\alpha e^2\epsilon)^{1/2} + \epsilon R_N^2 + \ldots]\,, \quad (4a)$$

and, for a neutral or positively charged system (Coulomb long-range potential), as

$$L_{\max}^2(\epsilon) = \left(\frac{2\mu}{\hbar^2}\right)[e^2 R_N + \epsilon R_N^2 + \ldots]\,, \quad (4b)$$

with μ and e, respectively, the mass and charge of the electron, and α the static polarizability of the cluster. Because of the low mass of the electron, Eq. (2) can be rewritten as

$$p(\epsilon) \propto L_{\max}^2(\epsilon)\exp(-\epsilon/kT)\,, \quad (5)$$

The most important difference between detachment and ionization arises from Eq. (4) since $L_{\max}$ [and, consequently, $p(\epsilon)$] vanishes for $\epsilon = 0$ in photodetachment while it remains finite in ionization. In the case of small size particles ($R_N \to 0$) the difference between Eqs. (1), (4a), and (4b) is dramatic. The dominant contribution to $p(\epsilon)$ in the limit ($R_N \to 0$) is proportional to $[\epsilon^{1/2}\exp(-\epsilon/kT)]$ in photodetachment and to $\exp(-\epsilon/kT)$ in photoionization. For a given temperature T, the maximum of $p(\epsilon)$ is found at $\epsilon_0 \approx \frac{1}{2}kT$ in photodetachment of a small negative cluster while $p(\epsilon)$ is maximum at $\epsilon_0 \approx kT$ in bulk matter. Photoelectron spectra are displayed in Fig. 2 for W_n^- clusters with $n = 4$–11 (bold line). Distributions calculated in the bulklike limit [dashed line—Eq. (1)] and according to Klots' formula [thin solid line—Eqs. (2) and (4a)] are compared with experimental results. In the low energy range (typically below 0.5 eV), the Klots' formula is in excellent agreement with the experiment, while the bulk formula predicts a distribution slightly shifted towards higher energy. The agreement is particularly spectacular for larger sizes ($n = 8$–11). The microcanonical temperature T defined in Eq. (3) has been used as an approximation of the isokinetic temperature [15]. This does not make any

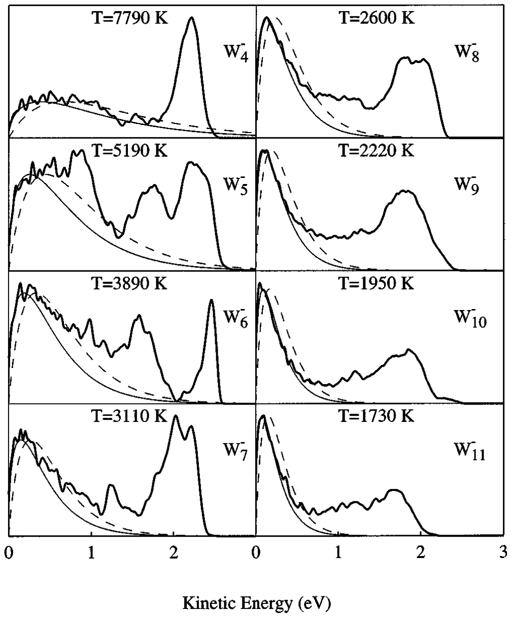

FIG. 2. Photoelectron kinetic energy spectrum obtained after image inversion for W_n^- clusters with $n = 4-11$ (thick solid line). The contribution of TE [Eqs. (2)–(4)] is plotted in the thin solid line. The dashed line corresponds to the bulk limit at the same temperature T [Eq. (1)]. Below 0.5 eV, the agreement between experiment and Klots's formula is remarkable. The remaining part of the spectrum is the contribution of direct photoemission.

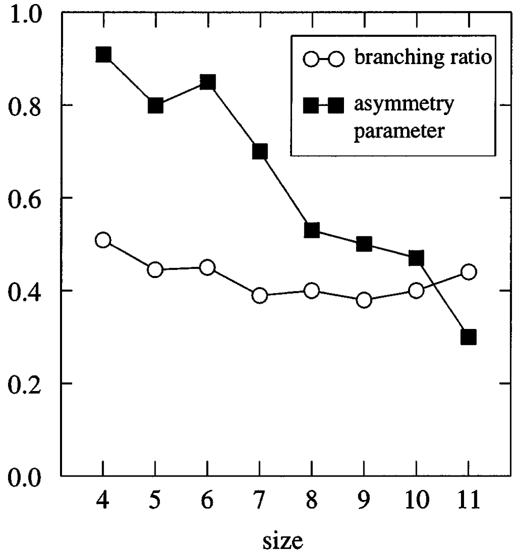

FIG. 3. Branching ratio $\rho_{\mathrm{TE}} = I_{\mathrm{TE}}/I_{\mathrm{total}}$ and asymmetry parameter β of the most intense band observed in DPE as a function of cluster size. In the range of $n = 4-11$, both decay processes are of comparable magnitudes ($\rho_{\mathrm{TE}} \approx 0.5$). The DPE of small systems is strongly anisotropic and aligned along the laser polarization axis ($\beta \approx 1$). It becomes more isotropic as the size of the system increases ($\beta \rightarrow 0$).

significant difference in the present case. We use the simplest expression for the static polarizability $\alpha = R_0^3$. The remaining part of the spectrum is the contribution from DPE which corresponds essentially to the building up of the d–valence band of tungsten. In Refs. [4,5], part of the broad difference between the total spectrum and the TE was attributed to inelastic electron scattering. This interpretation was based on the wrong argument that $p(\epsilon) \propto \exp(-\epsilon/kT)$ was valid for negative clusters. The correct expression derived from [15] is in excellent agreement with our experimental results, and theoretical predictions avoid the need to invoke an additional decay process. Our experiments have been conducted under low laser fluence in order to avoid multiphoton processes. More precisely, photoelectron spectra are recorded in the linear regime, where the shape of the whole spectrum does not depend on the laser fluence. In every case, the temperature T corresponding to the absorption of a single photon reproduces the observed distribution.

The branching ratios between TE and DPE may be extracted from the experimental data. The ratio $\rho_{\mathrm{TE}} = I_{\mathrm{TE}}/I_{\mathrm{total}}$ is plotted in Fig. 3. In the range $n = 4-11$, both decay processes are of comparable magnitudes ($\rho_{\mathrm{TE}} = 0.5$) which is rather surprising since, at both limits (atom and bulk), this quantity vanishes: DPE dominates in atoms and dimers, and the temperature T goes to zero when n increases. This means that the probability for the excited electron to leave the cluster with or without interaction with the nuclear motion is comparable at an excess energy close to 2 eV (typical value of $h\nu - \mathrm{EA}$ in the case discussed here). Just above threshold, the dominant decay process is TE while DPE becomes comparable only well above threshold. On the other hand, in large systems, even though the internal temperature corresponding to the absorption of a single photon is lower, the ratio ρ_{TE} remains about the same, indicating that the increasing number of vibrational degrees of freedom is accompanied by an increase of the electron-phonon coupling.

In Fig. 3 we have also plotted the asymmetry parameter β of the most intense band observed in DPE for each cluster size. The general trend in the evolution of this parameter is a monotonic decrease with n. The DPE of small systems is strongly anisotropic and aligned along the laser polarization axis ($\beta \approx 1$). It becomes more isotropic as the size of the system increases ($\beta \rightarrow 0$). This probably indicates the loss of coherence induced by electron-electron collisions occurring in large systems prior to electron-phonon coupling.

In the present experiment, the residence time of the clusters in the interaction zone is in the range 0.1–1 μs so that only relatively fast processes are visible. Although not measurable in velocity map imaging, previous observations in standard imaging allow us to give an upper bound for the lifetime of the excited cluster with respect to TE. In every situation presented here, this lifetime is shorter than 100 ns. This time scale for thermionic "delayed" emission [24] is short as compared to those obtained, for example, in TE of neutral tungsten clusters [1–3] or fullerenes [8–12]. However, in the present case, the one-photon excitation occurs well above the detachment threshold, and the "fast" character of this delayed process is not in contradiction with the long lifetimes (several μs) associated with TE, observed when the excitation occurs just above threshold or following a multiphoton excitation process.

Our observation of TE as a dominant process competing with the DPE in the decay of negative clusters confirms that TE is the major slow photoelectron decay channel for refractory compounds. Our careful study of the kinetic energy distribution of threshold electrons shows that the thermal distribution cannot be described by a simple bulklike formula. On the contrary, our results are in excellent agreement with the more refined model of Klots [15]. Moreover, our results indicate that the transition towards a bulklike statistical behavior of the internal energy redistribution occurs very rapidly, as early as $n = 4$, owing to the high density of states in metallic clusters.

The "Laboratoire de Spectrométrie Ionique et Moléculaire" is a "Unité Mixte de Recherche CNRS-Université Lyon I" (UMR CNRS 5579).

---

[1] A. Amrein, R. Simpson, and P. Hackett, J. Chem. Phys. **94**, 4663 (1991).
[2] A. Amrein, R. Simpson, and P. Hackett, J. Chem. Phys. **95**, 1781 (1991).
[3] T. Leisner, K. Athanassenas, D. Kreisle, E. Recknagel, and O. Echt, J. Chem. Phys. **99**, 9670 (1993).
[4] H. Weidele, D. Kreisle, E. Recknagel, G. Shulze Icking-Konert, H. Handschuh, G. Ganteför, and W. Eberhardt, Chem. Phys. Lett. **237**, 425 (1995).
[5] G. Ganteför, W. Eberhardt, H. Weidele, D. Kreisle, and E. Recknagel, Phys. Rev. Lett. **77**, 4524 (1996).
[6] H. Weidele, S. Becker, H.J. Kluge, M. Lindinger, L. Schweikhard, C. Walther, J. Ziegler, and D. Kreisle, Surf. Rev. Lett. **3**, 541 (1996).
[7] B.A. Collings, A.H. Amrein, D.M. Rayner, and P.A. Hackett, J. Chem. Phys. **99**, 4174 (1993).
[8] L.S. Wang, J. Conceicao, C. Jin, and R.E. Smalley, Chem. Phys. Lett. **182**, 5 (1991).
[9] E.E.B. Campbell, G. Ulmer, and I.V. Hertel, Phys. Rev. Lett. **67**, 1986 (1991).
[10] Y. Zhang and M. Stuke, Phys. Rev. Lett. **70**, 3231 (1993).
[11] J.U. Andersen, C. Brink, P. Hvelplund, M.O. Larsson, B. Bech Nielsen, and H. Shen, Phys. Rev. Lett. **77**, 3991 (1996).
[12] K. Hansen and O. Echt, Phys. Rev. Lett. **78**, 2337 (1997).
[13] N.W. Ashcroft and N.D. Mermin, *Solid State Physics* (Saunders, London, 1976).
[14] G. Ertl and J. Küppers, *Low Energy Electrons and Surface Chemistry* (VCH, Weinheim, 1985).
[15] C.E. Klots, J. Chem. Phys. **90**, 4470 (1989); Z. Phys. D **20**, 105 (1991); Chem. Phys. Lett. **186**, 73 (1991); J. Chem. Phys. **98**, 1110 (1993); J. Chem. Phys. **100**, 1035 (1994).
[16] C.E. Klots and R.N. Compton, Surf. Rev. Lett. **3**, 535 (1996).
[17] P. Kruit and F.H. Read, J. Phys. E **16**, 313 (1983).
[18] H. Helm, N. Bjerre, M. Dyer, D. Huestis, and M. Saeed, Phys. Rev. Lett. **70**, 3221 (1993).
[19] C. Bordas, M.J. Dyer, T. Fairfield, H. Helm, and K.C. Kulander, Phys. Rev. A **51**, 3726 (1995).
[20] C. Bordas, F. Paulig, H. Helm, and D.L. Huestis, Rev. Sci. Instrum. **67**, 2257 (1996)
[21] D.H. Parker and A.T.J.B Eppink, J. Chem. Phys. **107**, 2357 (1997).
[22] A.T.J.B Eppink and D.H. Parker, Rev. Sci. Instrum. **68**, 3477 (1997).
[23] J.C. Pinaré, B. Baguenard, C. Bordas, and M. Broyer (to be published).
[24] F. Remacle and R.D. Levine, Phys. Lett. A **173**, 284 (1993).